Electronic Supplementary Material (ESI) for Lab on a Chip.

Supporting Information

Ordered surface crack patterns *in situ* formed under confinement on fluidic microchannel boundaries in polydimethylsiloxane

Yang Bu,[a] Sheng Ni,[a] and Levent Yobas[*ab]*

[a]Department of Electronic and Computer Engineering,

[b]Division of Biomedical Engineering,

The Hong Kong University of Science and Technology,

Clear Water Bay, Hong Kong SAR, China.

[*]E-mail: eelyobas@ust.hk

Supporting Figures

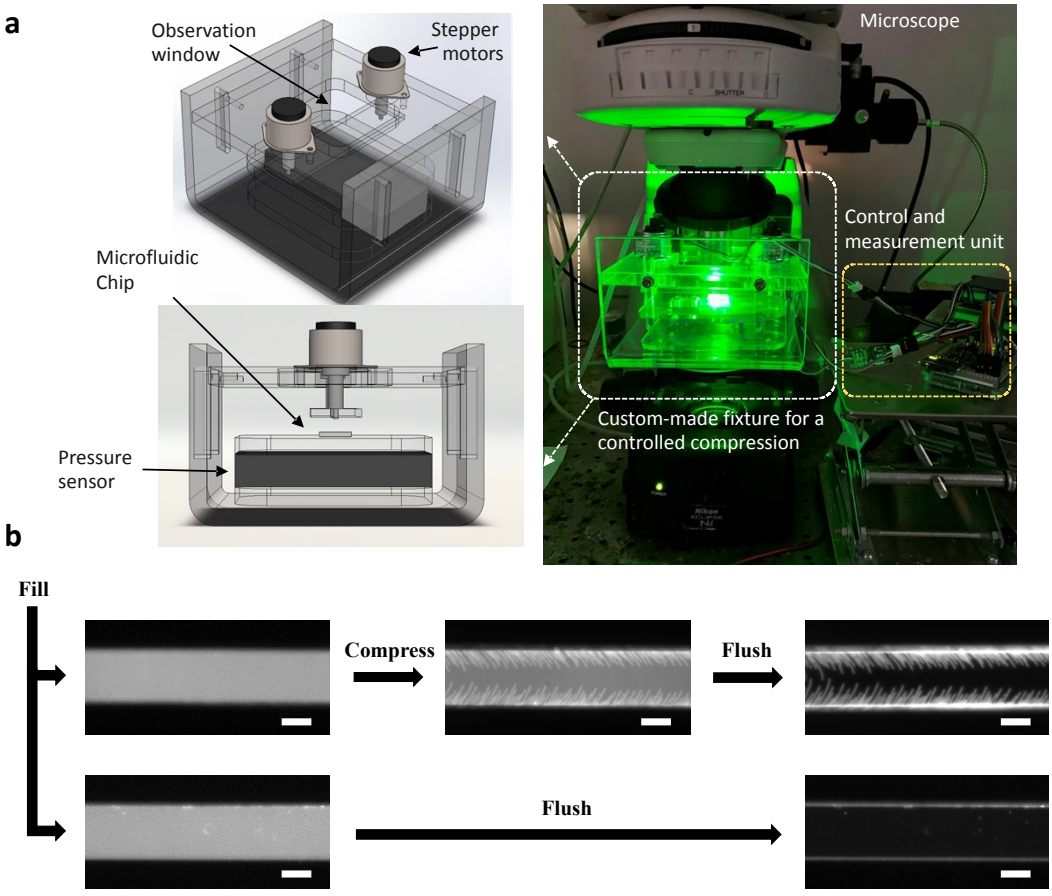

Fig. S1 (a) Picture: experimental setup used for fluorescent microscopy imaging of *in situ* crack formation on microfluidic channel boundaries in PDMS. Sketch: custom-made fixture featuring stepper motors and a pressure sensor driven by a microcontroller board for exerting a controlled compression. (b) Fluorescent images of straight channel segments loaded with 200 nm polystyrene spheres shown before and after flushing with water. Above: surface cracks appear after an externally applied uniaxial compression. Below: no visible crack pattern can be found without any compression applied, indicating that cracks are not caused by the oxygen plasma treatment applied at 29.6 W for 90 s. Microchannel width: 100 µm; depth: 35 µm. Scale bars: 50 µm.

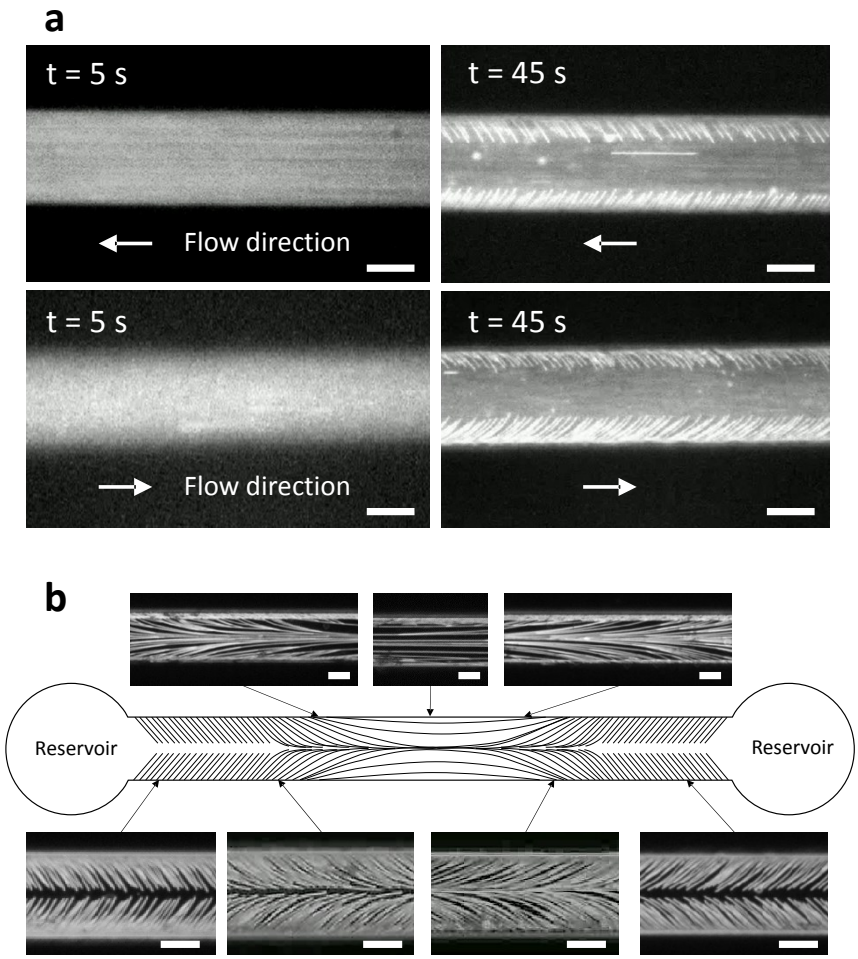

Fig. S2 (a) Fluorescent images of channel segments underwent 30 N compression before exposure to liquid. The images show the segments 5 and 45 s after the onset of flushing with aqueous suspension of 200 nm polystyrene spheres. The segments that are shown in upper and lower rows (under opposite flush directions) refer to the corresponding sections of identical channels and thus exhibit patterns with comparable tilt angles. (b) Schematic description of crack patterns observed along a straight channel and their position-dependent variation, presented together with respective fluorescent images (channel segments). The channel similarly underwent 30 N compression before exposure to liquid, followed by a sequence of wash steps with aqueous suspension of 200 nm polystyrene spheres and then water before imaging. The oxygen plasma treatment applied at 29.6 W for 90 s. Microchannel width: 100 μm; depth: 35 μm. Scale bars: 50 μm.

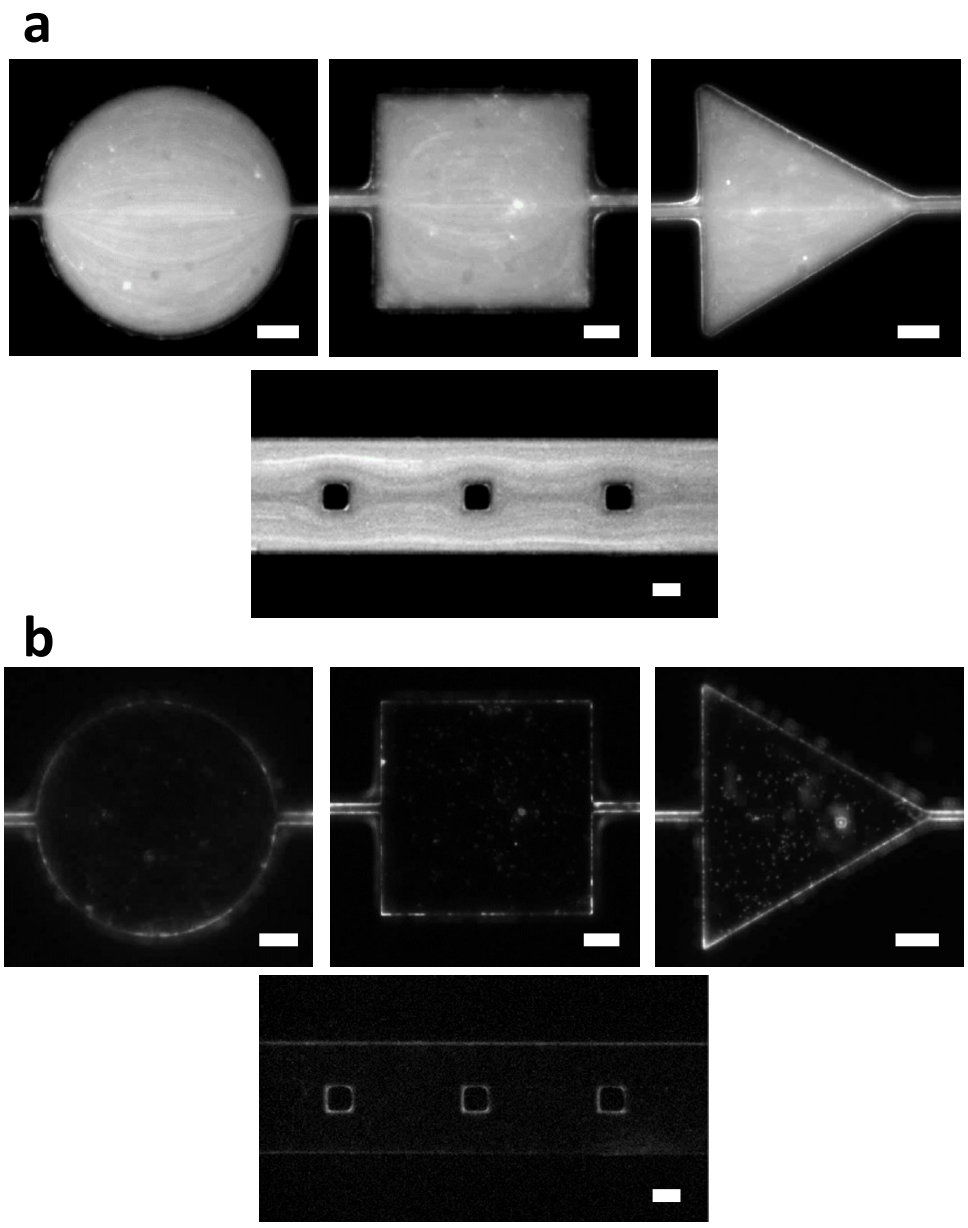

Fig. S3 Fluorescent images of chambers and a channel segment featuring square pillars, all with no compression history. The images show the chambers and the segment (a) 10 min after the onset of flushing with aqueous suspension of 200 nm polystyrene spheres as well as (b) after a water flush. No significant pattern can be observed as the specimens did not undergo compression. Scale bars: 50 μm.

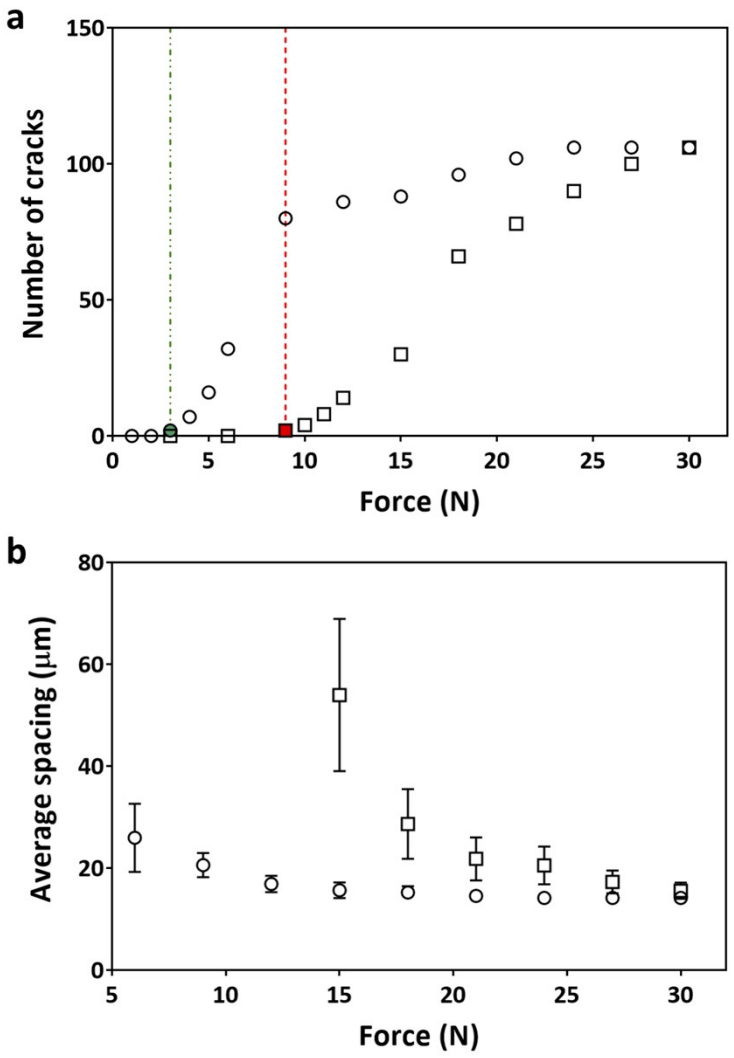

Fig. S4 (a) Plots showing the number of cracks and (b) average spacing between cracks as a function of compression delivered at step increments of 0.5 N in 1-s (squares) or 15-s intervals (circles). Red and green vertical dashed lines mark respective force threshold levels when cracks begin to appear.

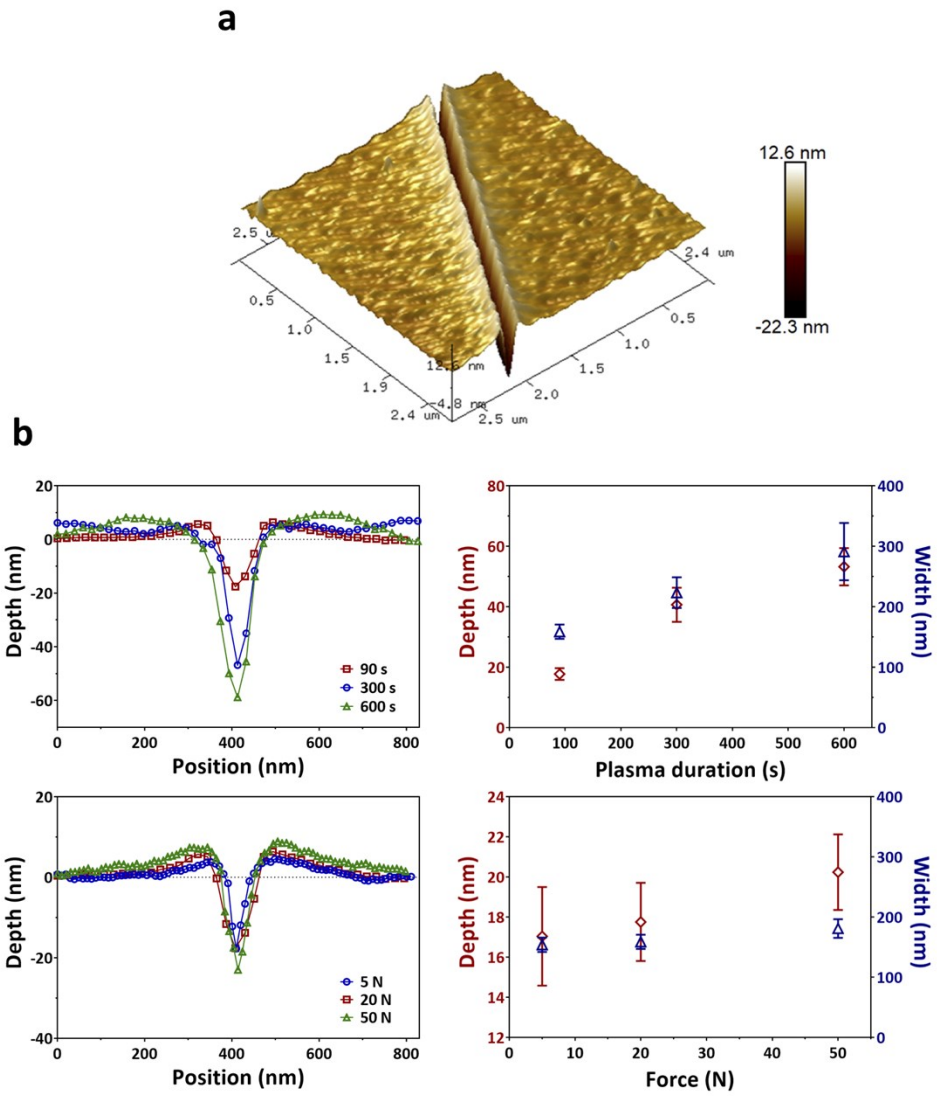

Fig. S5 AFM measurements of surface cracks: (a) 3D profile of a representative crack. (b) Plots: crack depth profiles as well as crack depth and width average values obtained with varying oxygen plasma treatment durations and compression strengths (legends). Error bars: ±1 s.d. ($n = 5$). Unless otherwise stated, the channels underwent 30 N compression subsequent to a 90-s exposure to oxygen plasma treatment at 29.6 W. The measurements in tapping mode were carried out using a Dimension Icon® (Bruker, Germany) AFM with an aluminum-coated silicon nitride probe (SCANASYST-AIR, Bruker), having a nominal spring constant of 0.4 N/m, a resonant frequency of 70 kHz and a tip radius of 2 nm. Scans of 5 × 5 μm areas were performed with a scan rate at 1 Hz and 512 sample points/line. Images were processed with NanoScope Analysis Software (Bruker, Germany).

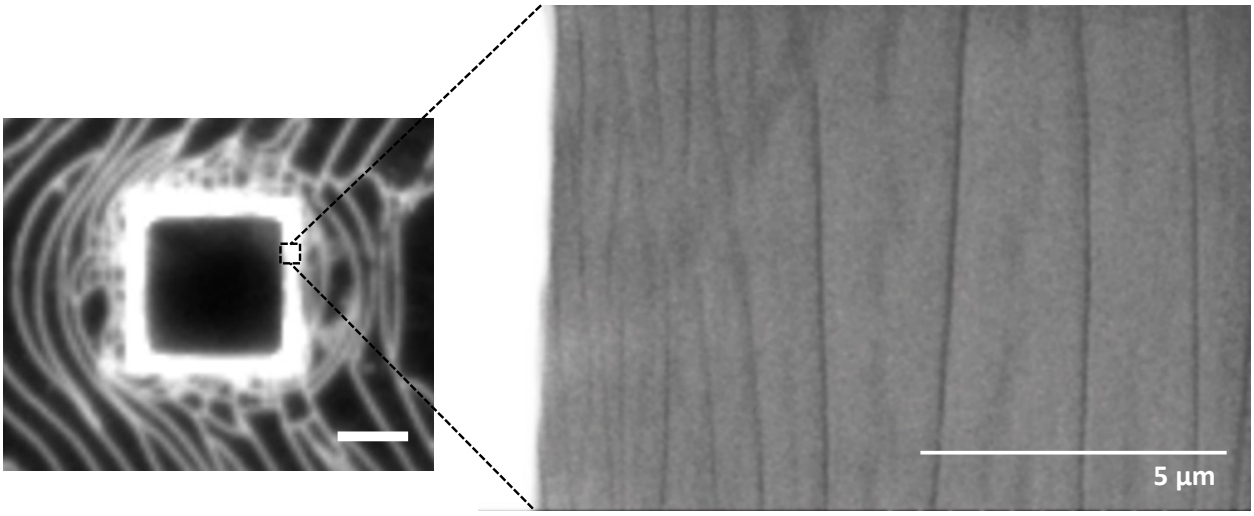

Fig. S6 Scanning electron micrograph revealing a dense pattern of surface cracks on PDMS top channel boundary surrounding a square post responsible for the rim of high fluorescence intensity. Scale bars: 25 µm (fluorescent image) and 5 µm (electron micrograph).

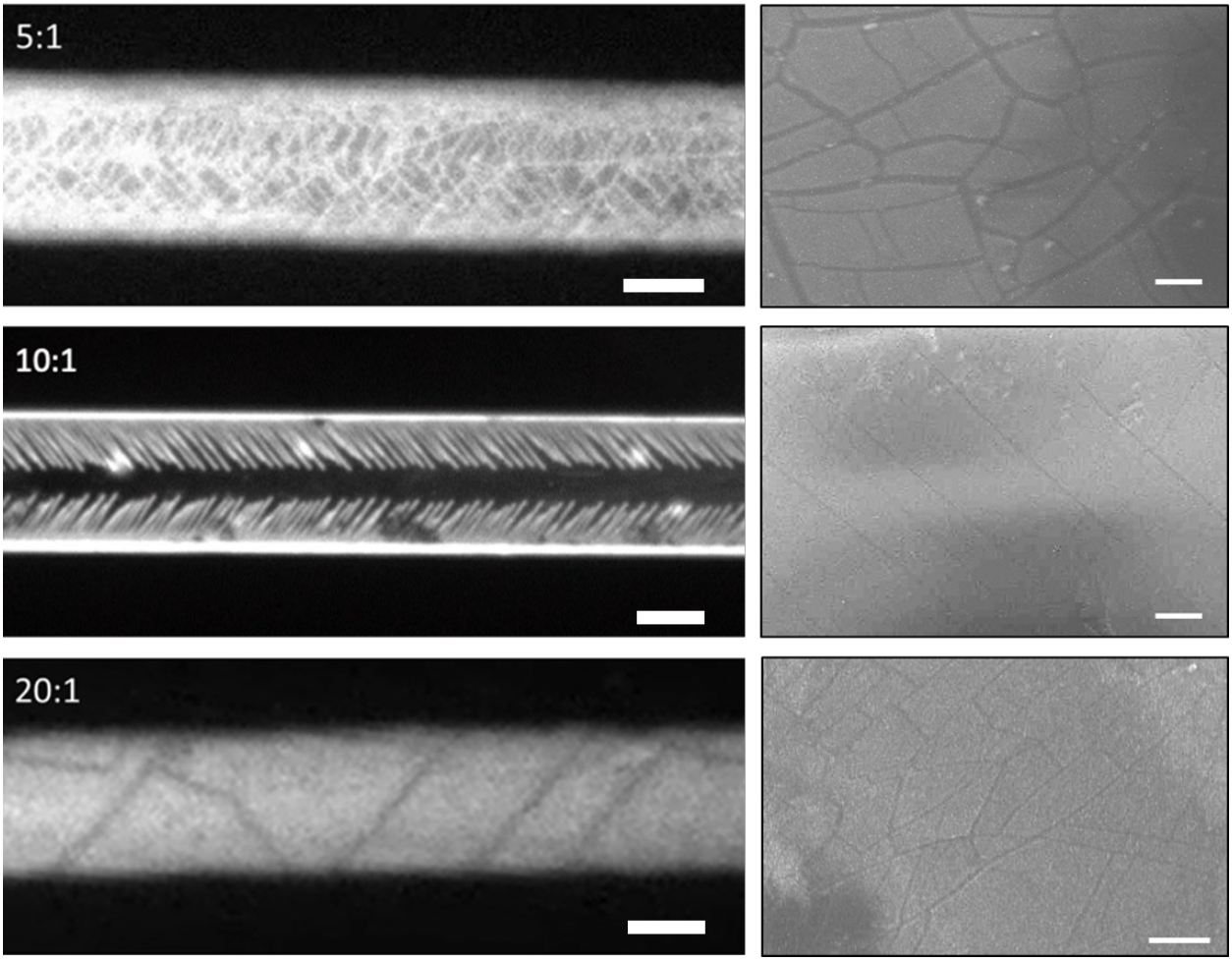

Fig. S7 Fluorescent images of straight channel segments and accompanying electron micrographs (top channel boundaries) reveal disordered surface crack patterns in "hard" and "soft" PDMS replicas in relation to ordered crack patterns in "default" replica prepared at the material base:curing agent weight ratio of 5:1, 20:1 and 10:1, respectively. Microchannel width: 100 μm; depth: 35 μm. Scale bars: 50 μm (fluorescent images) and 2 μm (electron micrographs).

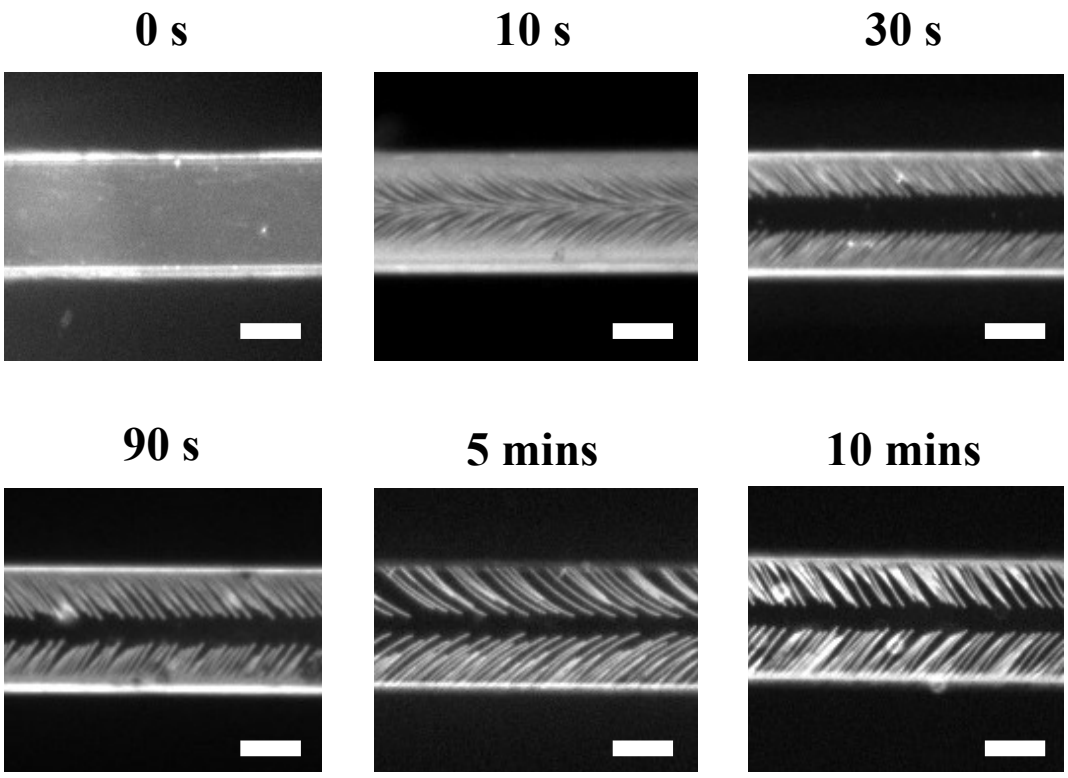

Fig. S8 Fluorescent images of straight channel segments show the resultant crack patterns in relation to the duration of oxidation (oxygen plasma treatment time). Microchannel width: 100 μm; depth: 35 μm. Scale bars: 50 μm.

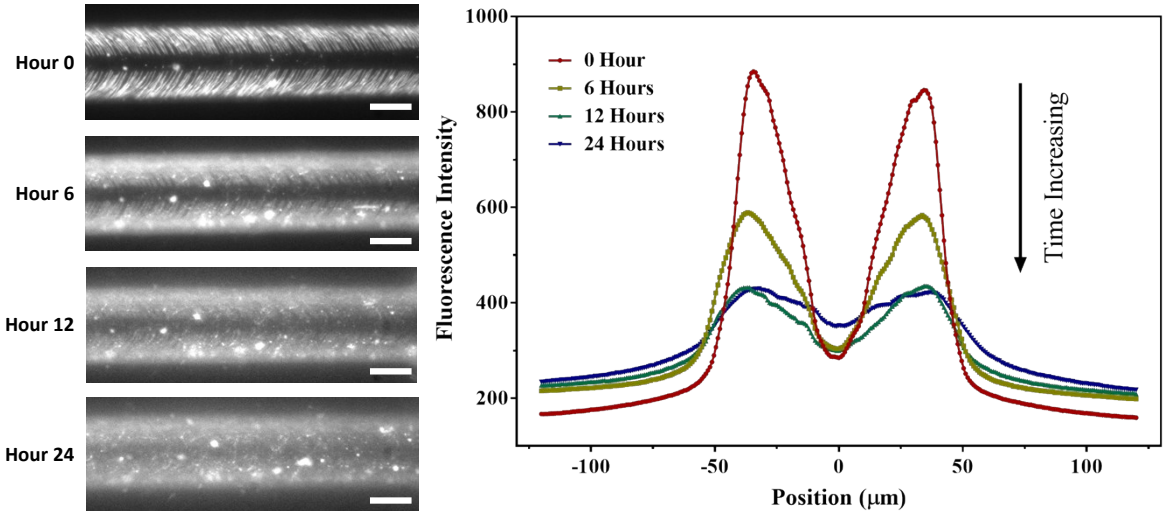

Fig. S9 Fluorescent images of a straight channel segment featuring surface cracks show the evolution of fluorescent patterns over time since the time of compression (during the recovery of surface hydrophobicity). Plot of the corresponding fluorescent intensity across the channel width with the origin taken as the channel center. Microchannel width: 100 μm; depth: 35 μm. Scale bars: 50 μm.

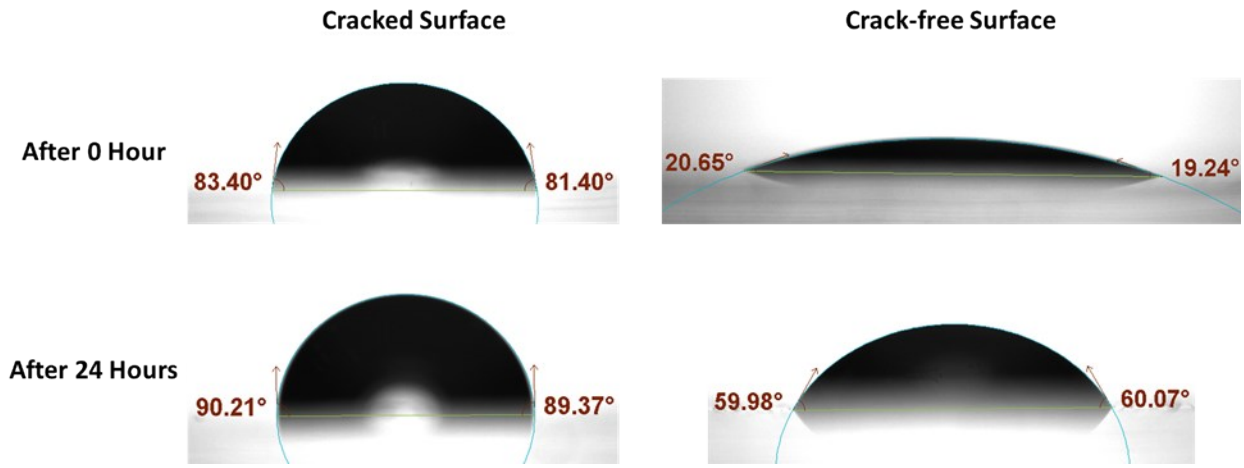

Fig. S10 Surface contact angles on PDMS specimens measured with and without compression-induced surface cracks immediately after the time of compression and also after a recovery period of 24 h.

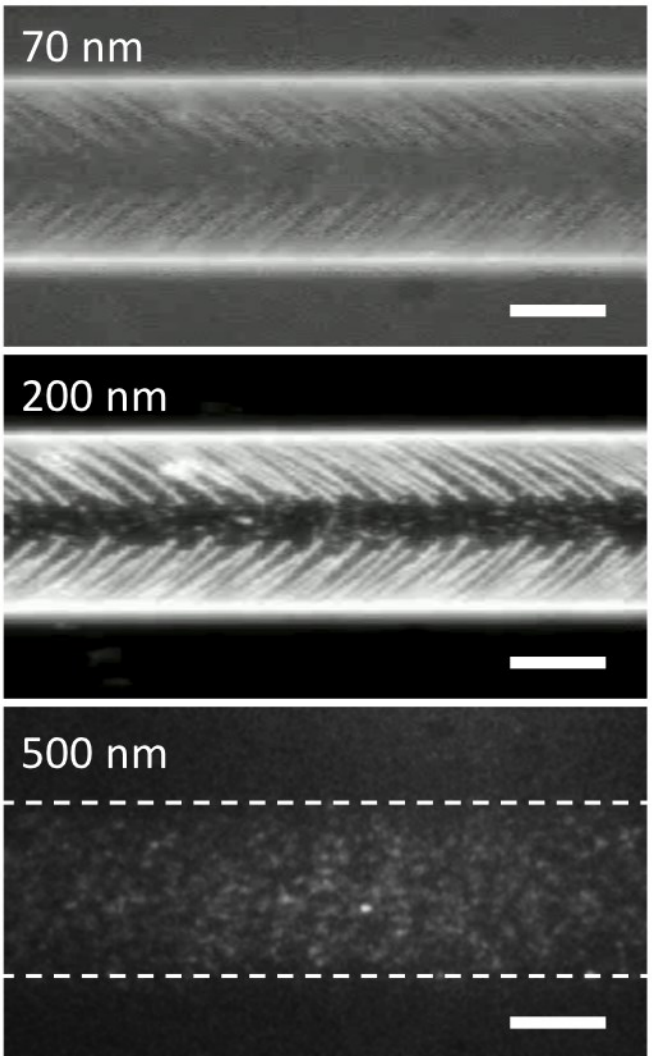

Fig. S11 (a) Fluorescent images of a channel segment featuring surface cracks during flushing with a triphasic aqueous suspension of 70, 200, and 500 nm polystyrene spheres. The crack pattern becomes visible only through the filter sets respective of 70 and 200 nm particles, suggesting that 500 nm particles are excluded from cracks and thus a channel with surface cracks serve as a filter. Microchannel width: 100 μm; depth: 35 μm. Scale bars: 50 μm.